Published in final edited form as:

Cancer Discov. 2013 January ; 3(1): 68–81. doi:10.1158/2159-8290.CD-12-0049.

Loss of 53BP1 Causes PARP Inhibitor Resistance in *Brca1*-Mutated Mouse Mammary Tumors

Janneke E. Jaspers[1,2], **Ariena Kersbergen**[1], **Ute Boon**[2], **Wendy Sol**[1], **Liesbeth van Deemter**[1], **Serge A. Zander**[1], **Rinske Drost**[2], **Ellen Wientjens**[2], **Jiuping Ji**[3], **Amal Aly**[5], **James H. Doroshow**[4], **Aaron Cranston**[6], **Niall M.B. Martin**[6], **Alan Lau**[7], **Mark J. O'Connor**[7], **Shridar Ganesan**[5], **Piet Borst**[1], **Jos Jonkers**[2], **Sven Rottenberg**[1]

[1]Division of Molecular Oncology, The Netherlands Cancer Institute, Amsterdam, the Netherlands [2]Division of Molecular Pathology, The Netherlands Cancer Institute, Amsterdam, the Netherlands [3]National Clinical Target Validation Laboratory, National Cancer Institute, Frederick [4]Division of Cancer Treatment and Diagnosis and Laboratory of Molecular Pharmacology, National Cancer Institute, Bethesda, Maryland [5]Cancer Institute of New Jersey, New Brunswick, New Jersey [6]KuDOS Pharmaceuticals, Cambridge [7]AstraZeneca, Macclesfield, United Kingdom

Abstract

Inhibition of PARP is a promising therapeutic strategy for homologous recombination–deficient tumors, such as BRCA1-associated cancers. We previously reported that BRCA1-deficient mouse mammary tumors may acquire resistance to the clinical PARP inhibitor (PARPi) olaparib through activation of the P-glycoprotein drug efflux transporter. Here, we show that tumor-specific genetic inactivation of P-glycoprotein increases the long-term response of BRCA1-deficient mouse mammary tumors to olaparib, but these tumors eventually developed PARPi resistance. In a fraction of cases, this resistance is caused by partial restoration of homologous recombination due to somatic loss of 53BP1. Importantly, PARPi resistance was minimized by long-term treatment with the novel PARP inhibitor AZD2461, which is a poor P-glycoprotein substrate. Together, our

Corresponding Authors: Jos Jonkers, Division of Molecular Pathology, Netherlands Cancer Institute, Plesmanlaan 121, 1066 CX Amsterdam, the Netherlands. Phone: 31-20-512-2000; Fax: 31-20-669-1383; j.jonkers@nki.nl; and Sven Rottenberg, s.rottenberg@nki.nl.

Current address for A. Cranston: Precos Ltd., In vivo services, Loughborough, United Kingdom; and current address for N.M.B. Martin: Mission Therapeutics, Cambridge, United Kingdom

Authors' Contributions

Conception and design: J.E. Jaspers, A. Aly, N.M.B. Martin, M.J. O'Connor, S. Ganesan, P. Borst, J. Jonkers, S. Rottenberg

Development of methodology: J.E. Jaspers, L. van Deemter, R. Drost, J. Ji, A. Cranston, A. Lau, P. Borst, J. Jonkers, S. Rottenberg

Acquisition of data (provided animals, acquired and managed patients, provided facilities, etc.): J.E. Jaspers, A. Kersbergen, W. Sol, L. van Deemter, S.A.L. Zander, R. Drost, J. Ji, A. Aly, J.H. Doroshow, A. Cranston, A. Lau, S. Rottenberg

Analysis and interpretation of data (e.g., statistical analysis, biostatistics, computational analysis): J.E. Jaspers, J. Ji, A. Cranston, N.M.B. Martin, S. Ganesan, J. Jonkers, S. Rottenberg

Writing, review, and/or revision of the manuscript: J.E. Jaspers, R. Drost, A. Aly, J.H. Doroshow, M.J. O'Connor, S. Ganesan, P. Borst, J. Jonkers, S. Rottenberg

Administrative, technical, or material support (i.e., reporting or organizing data, constructing databases): J.E. Jaspers, A. Kersbergen, U. Boon, W. Sol, S.A.L. Zander, R. Drost, E. Wientjens, A. Lau, S. Rottenberg

Study supervision: A. Cranston, A. Lau, P. Borst, J. Jonkers, S. Rottenberg

Disclosure of Potential Conflicts of Interest

A. Cranston, N.M.B. Martin, A. Lau, and M.J. O'Connor were employees of KuDOS Pharmaceuticals, which developed olaparib and AZD2461. A. Lau and M.J. O'Connor are currently employees of AstraZeneca.

Note: Supplementary data for this article are available at Cancer Discovery Online (http://cancerdiscovery.aacrjournals.org/).

data suggest that restoration of homologous recombination is an important mechanism for PARPi resistance in BRCA1-deficient mammary tumors and that the risk of relapse of BRCA1-deficient tumors can be effectively minimized by using optimized PARP inhibitors.

INTRODUCTION

Inhibition of PARP1 induces synthetic lethality in cells that are defective in homologous recombination (HR) due to loss of BRCA1 or BRCA2 or other HR-associated proteins (1–3). PARP1 inhibition results in unrepaired DNA single-strand breaks (SSB), which are eventually converted into double-strand breaks (DSB) during DNA replication. Although HR-proficient cells can repair these DSBs in an error-free manner, HR-deficient cells cannot, and die. Preclinical studies and phase I and II clinical trials have shown potent antitumor efficacy of the PARP inhibitor (PARPi) olaparib (AZD2281) as a single agent in BRCA1- or BRCA2-associated cancers, with only modest side effects (4–10). Unfortunately, not all patients with cancer who carry *BRCA1* or *BRCA2* mutations respond to PARPi therapy (4, 10), which is impeding further clinical development of this promising therapeutic approach. Identification of the mechanisms underlying PARPi resistance is therefore important for improving treatment and for prediction of tumor response before treatment.

Because pre- or post-PARPi treatment tumor samples from patients with BRCA1-deficient cancers are still limited, we studied the response and resistance to the clinical PARPi olaparib in a validated genetically engineered mouse model for *BRCA1*-mutated breast cancer (9, 11, 12). Mammary tumors that arise in these mice were highly sensitive to olaparib (9). Nevertheless, long-term olaparib response was frequently hampered by increased expression of the *Mdr1a/b* (also known as *Abcb1a/b*) genes, which encode the drug efflux transporter P-glycoprotein (Pgp; ref. 9). In addition, the MRE11A-deficient human colon cancer cell line HCT-15, which expresses Pgp, could be sensitized to olaparib by combining it with the Pgp inhibitor verapamil (Oplustilova et al., unpublished data). However, the relevance of Pgp in clinical drug resistance is still controversial, and there may be a difference in the induction of Pgp expression between mice and humans (13).

Recently, we have also shown that mouse mammary tumors that contain the $Brca1^{C61G}$ mutation still show hypomorphic BRCA1 activity that explains the modest responses to olaparib or cisplatin treatment (14). With use of BRCA2-deficient cell lines, another PARPi resistance mechanism has previously been identified: Genetic reversion of the *BRCA2* mutation causes resistance to PARP inhibition or cisplatin (15, 16). Secondary mutations that restore BRCA1/2 function have subsequently been found in platinum-resistant hereditary ovarian cancers (17, 18).

Here, we set out to identify novel mechanisms of PARPi resistance that cannot be explained by Pgp-mediated drug efflux, residual BRCA1 activity, or restoration of BRCA1 function. For this purpose, we have used a mouse model in which mammary tumors arise that contain a large, irreversible *Brca1* mutation on a Pgp-deficient background. We report on inactivation of p53-binding protein 1 (53BP1) as a causal factor in PARPi resistance, and on

the successful circumvention of drug resistance of Pgp-proficient tumors using AZD2461, a novel PARPi with lower affinity to Pgp.

RESULTS

Elimination of Pgp Prolongs the Response of BRCA1-Deficient Mouse Mammary Tumors to Olaparib, but Tumors Still Develop Drug Resistance

Using the *K14cre;Brca1*$^{F/F}$*;p53*$^{F/F}$ (KB1P) mouse model for BRCA1-associated breast cancer, we have previously shown that activation of Pgp induces resistance to the PARPi olaparib (9). To study olaparib sensitivity of KB1P mammary tumors in the absence of functional Pgp, we bred the *Mdr1a/b* null alleles (19, 20) to homozygosity into our KB1P model (Supplementary Fig. S1A). Eleven individual mammary tumors from *K14cre;Brca1*$^{F/F}$*;p53*$^{F/F}$*;Mdr1a/b*$^{-/-}$ (KB1PM) mice were orthotopically transplanted into syngeneic FVB mice, which were subsequently treated with olaparib and monitored for survival (Fig. 1A and Supplementary Fig. S1B). All tumors were initially highly sensitive to olaparib. Moreover, the response of tumors derived from the same original donor tumor was comparable (Supplementary Fig. S2), showing that initial heterogeneity in PARPi response is limited. The survival of mice bearing Pgp-deficient KB1PM tumors increased compared with mice carrying Pgp-proficient KB1P tumors, following 28 days of treatment with olaparib ($P = 0.0392$, Fig. 1A and Supplementary Fig. S1B and S1C). This result confirms that Pgp plays a pivotal role in the development of olaparib resistance in the KB1P model, as we have shown previously using the Pgp inhibitor tariquidar (9). Despite this increased survival, all mice eventually developed tumor recurrences that no longer responded to olaparib (Supplementary Fig. S1B). Because of the large intragenic deletion of *Brca1* in our model (11), PARPi resistance cannot be caused by restoration of BRCA function, as was found previously for BRCA2-deficient CAPAN1 cells (15). Hence, PARPi resistance can arise *in vivo* in the absence of 2 known resistance mechanisms: drug efflux by Pgp and genetic reversion of the *Brca1* mutation.

The Characteristics of Olaparib-Resistant KB1PM Tumors Suggest Activation of DNA Damage Repair

We transplanted 9 individual olaparib-resistant KB1PM tumors into syngeneic mice and found that the resistance was stable (Fig. 1B). To exclude that olaparib resistance in KB1PM tumors is driven by alterations of the drug target PARP resulting in restoration of poly(ADP-ribose) (PAR) formation, we tested the effects of olaparib on PARP activity in control versus olaparib-resistant tumors from 3 different donors (Fig. 1C). PAR levels were low or undetectable in olaparib-resistant tumors 30 minutes after olaparib administration and after 7 days of daily treatment with olaparib, showing that PARP function is still inhibited by olaparib, thus excluding alteration of the drug target as a PARPi resistance mechanism. As a consequence of the inhibition of PARP activity in both control and olaparib-resistant tumors, DNA DSBs have increased, as measured by γ-H2AX staining (Supplementary Fig. S3).

To test whether the sensitivity to DNA damage inflicted by other DNA-targeting anticancer drugs would also be altered, we transplanted olaparib-resistant and corresponding control tumors from 5 individual KB1PM donors. The tumor-bearing mice were treated with the

topoisomerase I inhibitor topotecan, the DNA adduct–forming agent cisplatin, or the topoisomerase II inhibitor doxorubicin. Almost all drug-naïve KB1PM tumors responded well to cisplatin or doxorubicin, and about half of the tumors showed high topotecan sensitivity (Fig. 2A). In contrast, none of the olaparib-resistant KB1PM tumors shrank more than 50% following treatment with topotecan (Fig. 2A and B). Although olaparib-resistant KB1PM tumors were usually still sensitive to cisplatin or doxorubicin, the time to relapse of these tumors was reduced in comparison with that of the drug-naïve KB1PM tumors (Fig. 2C and D). The fact that olaparib-resistant KB1PM tumors are cross-resistant to topotecan and recover more quickly from cisplatin- or doxorubicin-mediated DNA damage supports the hypothesis that olaparib-resistant KB1PM tumors have an altered DNA damage response compared with that in control tumors.

Loss of 53BP1 Causes Olaparib Resistance by Restoration of HR

We and others have recently identified 53BP1 as a factor for maintaining the growth defect of *Brca1*-deficient cell lines (21, 22). Loss of 53BP1 partially restores HR in BRCA1-deficient cells, thereby reducing their hypersensitivity to PARP inhibition and DNA-damaging agents. Using immunohistochemistry, we tested whether 53BP1 was lost in any of our KB1PM tumors, which acquired olaparib resistance *in vivo*. We found that 3 of 11 olaparib-resistant KB1PM tumors at least partly lost 53BP1 protein, whereas all untreated KB1PM tumors were positive (Fig. 3A and B). Besides these differences between individual olaparib-resistant tumors, we also observed intratumor heterogeneity: 53BP1-positive and -negative cell nests were both present in olaparib-resistant tumors KB1PM3 (Fig. 3B) and KB1PM8 (data not shown). In 2 olaparib-resistant KB1PM tumors, we identified somatic mutations in the *Trp53bp1* gene that explain the loss of 53BP1 protein. We found 2 genomic rearrangements in olaparib-resistant KB1PM5 in intron 24 of *Trp53bp1* (Supplementary Fig. S4A and S4B). By cDNA sequencing, however, we detected only a duplication of exons 25 and 26 (Fig. 3C and Supplementary Fig. S4C), indicating that the duplication of a part of exon and intron 24 leads to nonsense-mediated mRNA decay. The duplication of exons 25 and 26 results in a frame shift and premature stop codon (Fig. 3C). In the 53BP1-negative tumor nests of the olaparib-resistant KB1PM8, we detected a heterozygous mutation in exon 12 (Fig. 3D). cDNA sequencing showed only the truncating mutation Q626*, suggesting that the wild-type allele is silenced, possibly by promoter methylation.

To test whether HR is restored in 53BP1-deficient KB1PM tumors, we derived cell lines from olaparib-sensitive and -resistant KB1PM5 tumors. The deletions of *Brca1*, *p53*, and *Mdr1* were confirmed by genotyping PCR (Supplementary Fig. S5A), and the array comparative genomic hybridization profiles of the cell lines resembled those of the original tumors (Supplementary Fig. S5B). Western blotting confirmed the complete lack of 53BP1 in the resistant cells, whereas it was still present in sensitive KB1PM5 cells (Supplementary Fig. S5C). In a clonogenic assay, the cell lines derived from the olaparib-resistant KB1PM5 tumor retained their resistance *in vitro* (Supplementary Fig. S5D). Importantly, we found that irradiation-induced RAD51 foci (IRIF) were present in olaparib-resistant KB1PM5 tumor cells, but absent in olaparib-sensitive KB1PM5 cells, indicating that DNA repair by HR is restored in 53BP1-deficient KB1PM tumors (Fig. 4A). However, the 53BP1-deficient KB1PM5 tumor cells did not contain as many RAD51 IRIFs as 53BP1- and BRCA1-

proficient KP3.33 cells (Fig. 4B), suggesting that HR restoration by 53BP1 loss in KB1PM tumors is only partial, which may explain the lack of cross-resistance to cisplatin and doxorubicin. In addition to the cell lines, we have analyzed the ability to form RAD51 IRIFs in short-term tumor cell cultures derived from 53BP1-negative olaparib-resistant KB1PM tumors and their controls (Fig. 4C). Olaparib-resistant tumor cells from KB1PM5 and KB1PM8 form RAD51 IRIFs and are negative for 53BP1 (Supplementary Fig. S6). Interestingly, olaparib-resistant tumor cells from the heterogeneous olaparib-resistant tumor KB1PM3 form RAD51 IRIFs, but also have functional 53BP1 in all cells tested, shown by the 53BP1 IRIFs. This finding indicates the presence of a 53BP1-independent mechanism of HR restoration in the 53BP1-positive tumor cell nests. In addition to KB1PM3, KB1PM5, and KB1PM8, we measured RAD51 and 53BP1 IRIFs in KB1PM1 and KB1PM9. Similar to KB1PM3, the olaparib-resistant cells of KB1PM9 form 53BP1 IRIFs, but also RAD51 IRIFs. Tumor cells derived from olaparib-resistant KB1PM1 have functional 53BP1 and do not show RAD51 IRIFs, indicating an HR-independent mechanism of PARPi resistance.

We next tested whether inactivation of 53BP1 is causal to PARPi resistance. To this end, we transduced 2 cell lines derived from an untreated KB1P tumor (KB1P-B11 and KB1P-G3) with lentiviral vectors encoding 2 individual short-hairpin RNAs (shRNA) against *Trp53bp1* (Fig. 5A). In these cell lines as well, depletion of 53BP1 partially restored the formation of RAD51 IRIFs (Supplementary Fig. S7A). A decrease of 53BP1 indeed resulted in reduced sensitivity to olaparib (Fig. 5B), indicating that 53BP1 loss causes olaparib resistance.

This notion was confirmed by experiments with the olaparib-resistant cell line KB1P-3.12, in which a point mutation in *Trp53bp1* intron 22 leads to a cryptic splice acceptor site before exon 23 and production of a frame-shifted mRNA (Supplementary Fig. S7B). When we reconstituted functional 53BP1 in this cell line, we observed increased olaparib sensitivity, further supporting the relevance of 53BP1 expression for olaparib sensitivity (Fig. 5C and D).

We also tested KB1P-B11 cells with stable shRNA-mediated depletion of 53BP1 *in vivo* after orthotopic transplantation of these cells in mice. The resulting outgrowths did not respond to olaparib anymore, whereas the control tumors were still sensitive (Fig. 5E). Immunohistochemical analysis confirmed the complete loss of 53BP1 expression in tumors derived from KB1P-B11 cells with stable 53BP1 depletion (Supplementary Fig. S7C). This finding directly proves that absence of 53BP1 in KB1P tumors is sufficient for complete resistance to olaparib. In line with our cross-resistance experiments (Fig. 2C), all tumor cell line outgrowths responded well to cisplatin treatment, but 53BP1-negative outgrowths tended to relapse earlier (Fig. 5F).

In view of the complete cross-resistance of olaparib-resistant tumors to topotecan (Fig. 2A and B), we tested whether loss of 53BP1 also contributes to drug resistance of tumors that were treated only with topotecan. Because the drug efflux transporter ABCG2 contributes to topotecan resistance of KB1P mouse mammary tumors (23), we used ABCG2-deficient KB1P tumors from *K14cre;Brca1*$^{F/F}$*;p53*$^{F/F}$*; Abcg2*$^{-/-}$ mice for these experiments. Indeed, we found that 53BP1 expression was absent in 3 of 20 topotecan-resistant tumors, whereas 53BP1 was still fully present in the corresponding tumors before treatment (Supplementary

Fig. S8). This observation strongly suggests that 53BP1 loss is not exclusively a mechanism of olaparib resistance but may also play a role in resistance to other commonly used anticancer agents.

Long-Term PARP Inhibition by AZD2461 Suppresses the Development of Resistance

To circumvent the development of PARPi resistance, we investigated whether long-term dosing of a PARPi would be capable of causing eradication or chronic suppression of KB1P tumors. We have previously shown that long-term olaparib treatment of 100 consecutive days significantly increased the overall survival of mice with KB1P tumors, compared with 28 days of treatment, but we also found that several of these tumors acquired Pgp-mediated resistance (9). Therefore, we tested the response of KB1P tumors to the novel PARPi AZD2461 (Supplementary Fig. S9A), which has lower affinity for Pgp than does olaparib (Oplustilova et al., unpublished data). Both AZD2461 and olaparib completely inhibited the PARP activity for several hours and the amount of PAR returned to baseline levels 24 hours, after treatment (Supplementary Fig. S9B). Six hours after drug administration, we observed a small difference in PARP activity. This difference may be caused by a higher potency of AZD2461 or a faster Pgp-mediated washout of olaparib. We confirmed the low affinity of AZD2461 to Pgp by testing the inhibitor on olaparib-resistant KB1P tumor T6–28, which has an 80-fold increased *Mdr1b* expression (9). This tumor is sensitized to olaparib by pretreatment with the Pgp inhibitor tariquidar, and it also responds well to AZD2461 without inhibition of Pgp (Fig. 6A). In contrast, Pgp-deficient olaparib-resistant KB1PM tumors do not respond to AZD2461 (Fig. 6B). These data show that AZD2461 is a novel PARPi with potential to bypass Pgp-mediated resistance to olaparib.

We first studied short-term AZD2461 treatment in mice with KB1P tumors, using daily dosing for 28 consecutive days, as we did for olaparib. Although mice treated with AZD2461 clearly showed increased survival compared with olaparibtreated mice ($P = 0.0061$), all mice eventually developed relapsing tumors that were refractory to PARPi treatment (Fig. 6C and Supplementary Fig. S9C). Three of 12 AZD2461-resistant KB1P tumors also showed loss of 53BP1 expression (Fig. 6D). In the AZD2461-resistant tumor KB1P2, we found a deletion of 94 base pairs in exon 21 of *Trp53bp1* (Fig. 6E and Supplementary Fig. S9D), which leads to a stop-codon in this exon. We also identified a deletion of 34 base pairs on the boundary of intron 24 and exon 25 of *Trp53bp1* in AZD2461-resistant tumor KB1P8 (Fig. 6F and Supplementary Fig. S9E).

When we increased the AZD2461 treatment to 100 consecutive days, we found that 8 of 9 mice engrafted with fragments from 3 individual KB1P tumors did not develop refractory tumors within 300 days after treatment start (Fig. 7A and Supplementary Fig. S10A–S10C). In contrast, 6 of 7 KB1P tumor-bearing mice that received 100 days of consecutive olaparib treatment acquired drug resistance in this time (Fig. 7A; ref. 9). The tumor that acquired AZD2461 resistance during the first treatment cycle had an epithelial-to-mesenchymal transition phenotype (Supplementary Fig. S10D), which is frequently linked to drug resistance (24).

Long-term AZD2461 treatment was well tolerated and doubled the median relapse-free survival from 64 to 132 days $P < 0.0001$, Fig. 7B). Intriguingly, long-term AZD2461

treatment did not result in tumor eradication: Although tumor remnants were not palpable during AZD2461 treatment, we found tumor relapse once treatment was stopped on day 100 (Supplementary Fig. S10A–S10C). Nevertheless, KB1P tumor recurrences were still sensitive when AZD2461 treatment was resumed.

DISCUSSION

Despite the induction of synthetic lethality of BRCA1-deficient cells by PARP inhibition (1, 2), a heterogeneous response of patients with breast or ovarian cancer who carry a *BRCA1* mutation has been observed recently (4, 10). This finding underscores the urgent need to identify mechanisms that thwart the success of this promising therapeutic approach. We have studied PARPi resistance using a mouse model for *BRCA1*-deleted breast cancer in which 2 known mechanisms, BRCA1 reexpression by genetic reversion and increased drug efflux by Pgp, were eliminated by genetic engineering. We show that loss of 53BP1 causes resistance to PARP inhibition in BRCA1-deficient mouse mammary tumors. As underlying mechanism, 53BP1-deficient KB1PM cells seem to have partially restored HR-mediated DNA repair, as evidenced by the presence of DNA damage–induced RAD51 foci. Hence, our data show that HR restoration by 53BP1 loss is a relevant drug resistance mechanism that occurs in real tumors.

Our results are consistent with recent *in vitro* data from Bunting and colleagues (22) and our own group (21) showing that 53BP1 loss in BRCA1-deficient cells increases resistance to DNA-damaging agents and partially restores HR activity. Although the underlying mechanisms are still under investigation, data from *in vitro* studies show that 53BP1 loss promotes end resection of DNA DSBs in the absence of BRCA1, resulting in RAD51 recruitment and subsequent HR (22). The importance of end resection for promoting HR over nonhomologous end joining (NHEJ) has been shown earlier (25–27).

Loss of 53BP1 adds a novel *in vivo* mechanism of PARPi resistance to 2 other resistance mechanisms that have previously been identified in preclinical models: restoration of BRCA function (15, 16, 18) and increased *Mdr1* gene expression (9). To what extent these mechanisms contribute to PARPi resistance in patients is still unclear, although secondary somatic mutations restoring BRCA1/2 function have been found in platinum-resistant hereditary ovarian cancers (18). Interestingly, 53BP1 expression is frequently absent in *BRCA1/2*-mutated or triple-negative breast cancers (21). We therefore hypothesize that the poor overall survival of patients with 53BP1-negative breast cancer (21) is partly due to increased resistance to DNA-damaging agents. It would therefore be useful to evaluate the use of 53BP1 as a biomarker for predicting response of BRCA1-deficient cancers to PARPi therapy.

HR restoration due to 53BP1 loss induces resistance not only to PARPi but also to the topoisomerase I inhibitor topotecan. In contrast, olaparib-resistant tumors were still sensitive to the DNA cross-linking agent cisplatin or the topoisomerase II inhibitor doxorubicin. Topotecan promotes SSBs that are converted into more cytotoxic DSBs during DNA replication. It is therefore conceivable that partial HR restoration is sufficient to antagonize

this effect. Moreover, the topotecan cross-resistance suggests that PARP inhibition primarily targets SSB repair (28).

Despite the remarkable capability of 53BP1-deficient cells to carry out homology-directed DNA repair in the absence of BRCA1, our data suggest that this restoration is not complete: The number of RAD51 IRIF-positive 53BP1-deficient KB1P(M) tumor cells does not reach the level observed in 53BP1- and BRCA1-proficient KP3.33 tumor cells *in vitro*. The fact that we observe more heterogeneous levels of RAD51 foci using the short-term cell cultures of tumor cell suspensions may be due to the more complex nature of this assay. Several factors in the procedure of tumor cell dissociation and subsequent adhesion to coverslips may have an impact on RAD51 foci quantification.

We have previously reported that the amount of DNA damage inflicted by olaparib is not sudden but accumulates over a short time (9). As a result, tumors shrink after only a few days of PARP inhibition, which correlates with a peak of y-H2AX foci about a week after the start of treatment. In contrast, the number of y-H2AX foci is much higher shortly after cisplatin treatment (data not shown). Hence, partial restoration of HR by 53BP1 loss may not be sufficient for BRCA1-deficient tumor cells to cope with the profound and acute induction of DNA damage by cisplatin. This lack of complete cross-resistance is consistent with the recent findings of Bunting and colleagues (30): The absence of 53BP1 in *Brca1*$^{\Delta 11/\Delta 11}$ mouse embryonic fibroblasts does not rescue the hypersensitivity to cisplatin, in contrast to the sensitivity to PARP inhibition. BRCA1 also has functions in interstrand crosslink repair that are not directly linked to the HR pathway, such as replication fork protection (30) or recruitment of FANCD2 (29, 31, 32). It is likely that such additional functions explain the partial sensitivity to cisplatin of our 53BP1- and BRCA1-deficient tumors.

The fact that 53BP1 loss occurs in only a fraction of PARPi-resistant mouse mammary tumors indicates that other resistance mechanisms should exist in 53BP1-positive tumors. These mechanisms might include impaired recruitment of 53BP1 to sites of DNA damage due to dysfunctional recruitment factors, such as RNF8 or RNF168, or prevention of PARPi-induced DNA damage through inhibition of other NHEJ-associated factors (33). We found at least 2 PARPi-resistant tumors (KB1PM3 and KB1PM9) in which both RAD51 and 53BP1 IRIFs are formed (Fig. 4C and Supplementary Fig. S6). This observation strongly suggests a 53BP1-independent mechanism of HR restoration in BRCA1-deficient cells. In addition, the lack of RAD51 IRIF formation in olaparib-resistant KB1PM1 suggests an HR-independent resistance mechanism. We are currently investigating what other mechanisms may explain this outcome by using functional screens in our panel of BRCA1-deficient cell lines.

The observation that in several PARPi-resistant tumors 53BP1 expression is lost in only a fraction of tumor cells strongly suggests that different resistance mechanisms may be selected within an individual tumor. Distinct clonal subpopulations and their relation to metastasis were recently characterized in breast cancer (34). Our data suggest that distinct subpopulations of tumor cells using different resistance mechanisms may evolve during PARPi treatment. This heterogeneity might complicate the design of novel therapeutic

strategies to reverse PARPi resistance. Our model may be a useful tool to test such therapeutic approaches before they enter clinical trials.

As one strategy to minimize the risk of developing PARPi resistance, we present continuous treatment with the novel PARPi AZD2461. Although 28-day treatment with AZD2461 resulted in induction of resistance (which was in several tumors mediated by 53BP1 loss), chronic treatment resulted in complete remission and suppression of refractory disease during a period of 300 days. Although chronic AZD2461 treatment did not result in tumor eradication, it inhibited the outgrowth of drug-resistant clones. Apparently, the pool of proliferating cells, in which new mutations can arise, is effectively reduced in size. Although we cannot exclude that resistance to AZD2461 may develop at later time points, our data suggest that chronic PARP inhibition may be a promising strategy to achieve long-term tumor suppression in patients with HR-deficient tumors. Other PARPis that are not Pgp substrates, such as veliparib (ABT888; ref. 35), might have the same potential. In case Pgp-mediated olaparib resistance does not occur in humans, stable disease suppression might also be achieved using olaparib. In fact, in a phase II study, maintenance therapy using olaparib prolonged progression-free survival of patients with high-grade serous ovarian carcinoma (36). Of note, benefit from long-term PARPi treatment may not be restricted to *BRCA*- mutation carriers, as 51% of the high-grade serous ovarian carcinomas were found to have a genetic or epigenetic alteration in the HR pathway and may therefore respond to PARPi (37).

Collectively, our results further the understanding of PARPi resistance and underscore the relevance of HR restoration in BRCA1-deficient mammary tumors that cannot escape treatment by increased drug efflux, restoration of BRCA1 function, or residual activity of the BRCA1-mutant protein (14). Moreover, we show how preclinical evaluation of targeted therapeutics in genetically engineered mice can facilitate the development of therapeutic strategies that may prolong the treatment benefit in patients with cancer.

METHODS

Mice, Generation of Mammary Tumors, and Orthotopic Transplantations

Brca1$^{\Delta/\Delta}$;*p53*$^{\Delta/\Delta}$ mammary tumors were generated in *K14-cre;Brca1*$^{F/F}$;*p53*$^{F/F}$ (KB1P) female mice and genotyped as described previously (11). In this study we used KB1P mice that were backcrossed to a pure FVB/N background. To generate *Brca1*$^{\Delta/\Delta}$;*p53*$^{\Delta/\Delta}$;*Mdr1a/b*$^{-/-}$ tumors, we crossed *Mdr1a/b*$^{-/-}$ mice (19, 20) with KB1P mice to produce *K14cre;Brca1*$^{F/F}$;*p53*$^{F/F}$;*Mdr1a/b*$^{-/-}$ (KB1PM) mice. *Mdr1a* and *Mdr1b* genotypes were tested by PCR with specific primers (*Mdr1a* forward: 5′-GTGCATAGACCACCCTCAAGG-3′; *Mdr1b* forward: 5′-AAGCTGTGCATGATTCTGGG-3′) for wild-type (*Mdr1a* reverse: 5′-GTCATGCACATCAAACCAGCC-3′; *Mdr1b* reverse: 5′-GAGAAAC-GATGTCCTTCCAG-3′) and deleted alleles (*Mdr1a* reverse: 5′-GGAGCAAAGCTGCTATTGGC-3′). Orthotopic transplantations into wild-type FVB/N mice, tumor monitoring, and sampling were conducted as described (12). For the transplantation of cell lines, 500,000 cells in PBS and Matrigel (1:1) were injected in the fourth right mammary fat pad. All experimental procedures on animals were approved by

the Animal Ethics Committee of The Netherlands Cancer Institute (Amsterdam, the Netherlands).

Drugs and Treatment of Tumor-Bearing Mice

Starting from 2 weeks after transplantation, tumor size was monitored at least 3 times a week. All treatments were started when tumors reached a size of approximately 200 mm^3. Olaparib (50 mg/kg intraperitoneally) and AZD2461 (100 mg/kg *per os*) were given for 28 consecutive days, unless otherwise indicated. If tumors did not shrink below 50% of the initial volume, treatment was continued for another 28 days; otherwise, a new treatment cycle of 28 days was started when the relapsing tumor reached a size of 100% of the original volume (except for Fig. 5E, in which only one 28-day cycle of olaparib treatment was used). AZD2461 was diluted in 0.5% w/v hydroxypropyl methylcellulose in deionized water to a concentration of 10 mg/mL. The synthesis of AZD2461 is described in international patent WO2009/093032, specifically compound number 2b. In brief, *O* -benzotriazol-1-yl-tetramethyluronium hexafluorophosphate (45.5 g, 119.86 mmol) was added by portion to a solution of 2-fluoro-5-((4-oxo-3,4-dihydrophthalazin-1-yl)methyl)benzoic acid (1) (27.5 g, 92.20 mmol), 4-methoxypiperidine (11.68 g, 101.42 mmol), and triethylamine (30.8 mL, 221.28 mmol) in dimethyl acetamide (450 mL) at 20°C under nitrogen. The resulting solution was stirred at 200°C for 21 hours. The solution was poured into water (2.5 L) and extracted with ethyl acetate [(EtOAc) 3 times]; then the combined extracts were washed with brine (3 times), dried ($MgSO_4$), filtered, and evaporated to a gum. The crude product was purified by flash silica chromatography, elution gradient 0% to 100% EtOAc in isohexane. Pure fractions were evaporated to dryness and slurred with EtOAc to afford 4-(4-fluoro3-(4-methoxypiperidine-1-carbonyl)benzyl)phthalazin-1(2H)-one (2b) (22.45 g, 61.6%) as a white solid after filtration and vacuum drying.

For testing cross-resistance, mice were given a single treatment regimen of topotecan (2 mg/kg intraperitoneally, days 0–4 and 14–18), cisplatin (Mayne Pharma, 6 mg/kg i.v., day 0), or doxorubicin (Amersham Pharmacia Netherlands, 5 mg/kg i.v., days 0, 7, and 14). Tariquidar (Avaant, 2 mg/kg intraperitoneally) was administered 15 minutes before the olaparib injection for 28 consecutive days. Tumor volume was calculated with the following formula: $l \times b^2 \times 0.5$.

PAR Immunoassay

The ELISA for detecting PAR was described before (38). In brief, tissue lysates were prepared in Cell Extraction Buffer (Invitrogen FNN0011) supplemented with ×1 Protease Inhibitor Cocktail (Sigma-Aldrich P-2714 or Roche 11697498001) and 2 mmol/L phenylmethylsulfonylfluoride (PMSF; Sigma-Aldrich, cat. no. 93482–50ML-F). Protein concentration was determined with BCA Protein Assay Kit (Thermo Scientific Pierce, cat. no. 23227 or 23225). PAR standards were prepared from pure PAR (BioMol International, SW-311) and diluted in SuperBlock (Pierce 37535). Pierce ReactiBind (15042) plates were coated with Trevigen Anti-PAR Polymer Monoclonal Antibody (4335) diluted to a concentration of 4 μg/mL in pH 9.6 carbonate buffer overnight at 4°C and washed with PBS–0.1% Tween (Sigma-Aldrich). Blocking was carried out with SuperBlock at 37°C for 1 hour. Samples, standards, and controls were incubated in the plate for 16 hours at 4°C. After

washing 4 times, rabbit anti-PAR (Trevigen 4336, 1:500 in PBS-2% BSA-1% mouse serum) was incubated at 25°C for 2 hours. Goat–anti-rabbit–horseradish peroxidase [HRP) KPL Inc.; 074–15-061, 1 μg/mL in PBS-2% BSA-1% mouse serum] was incubated at 25°C for 1 hour. Detection was conducted with SuperSignal Pico Chemiluminescent Substrate (Pierce 37070), and plates were read on a Tecan Infinite or Tecan GENios Pro Luminometer (Tecan; Mannedorf, Switzerland). Detailed descriptions of the sample preparation and the protocol are available online (39, 40).

Immunohistochemistry

For immunohistochemical stainings, antigen retrieval was done by cooking in citrate buffer pH 6.0 (53BP1 and γ-H2AX) or proteinase K digestion (vimentin). Furthermore, the stainings ware carried out by using 3% H_2O_2 for blocking endogenous peroxidase activity, 5% goat serum plus 2.5% bovine serum albumin (BSA) in PBS as blocking buffer and antibody diluent, overnight first-antibody incubation, and 1-hour incubation with the secondary antibody. For detection, we used streptavidin-HRP (Dako K1016, 10 minutes incubation at room temperature), DAB (Dako K3468), and hematoxylin counterstaining.

Immunoblotting

Cells were harvested by trypsinization, washed in PBS, lysed in radio-immunoprecipitation assay (RIPA) buffer (50 mmol/L Tris pH 7.5, 150 mmol/L NaCl, 1 mmol/L EDTA, 1% Nonidet P-40, 0.1% SDS, 0.5% Nadeoxycholate and 25× Complete Protease Inhibitor Cocktail; Roche), incubated on ice, and sonicated. Equal amounts of protein were run on NuPAGE Novex Tris-Acetate 3–8% (w/v; Invitrogen) according to the manufacturer's instructions, followed by Western blotting.

DNA Damage–Induced Foci Detection

Cryopreserved tumor pieces were digested with 3 mg/mL collagenase A and 0.1% trypsin for 2 hours at 37°C, filtered, seeded on coverslips, and irradiated with 10 Gy after 48 hours. Cell lines were grown on coverslips for 16 to 24 hours before irradiation. Cells were fixed 6 hours after irradiation in 2% paraformaldehyde in PBS^{++} (with 1 mmol/L $CaCl_2$ and 0.5 mmol/L $MgCl_2$). Cells were permeabilized in 0.2% Triton X-100/PBS^{++} for 20 minutes and incubated in staining buffer (1% BSA, 0.15% glycine, and 0.1% Triton X-100 in PBS^{++}) for 30 minutes at room temperature. The staining buffer was used for all washing steps and as a solvent for antibodies. Incubation with primary and secondary antibodies was done for 2 hours and 1 hour, respectively, at room temperature. DNA was stained with TO-PRO-3 (Molecular Probes, 1:2,000). Images were taken with a Leica TCS SP2 (Leica Microsystems) confocal system, equipped with an Ar Diode 561 and HeNe 633 laser system. Images were taken using a 63× NA 1.32 objective. Standard LCS software was used for processing. RAD51 foci were quantified by being counted in the maximum projection of z-images. At least 100 cells were counted blindly on 4 different fields per slide, and every cell line has been measured in 2 independent experiments.

Antibodies

All antibodies and their dilutions are summarized in Supplementary Table S1.

Establishment and Maintenance of Tumor Cell Lines

Tumors were harvested, minced, and digested in RPMI 1640 (Gibco) supplemented with 2% FBS (Sigma), 3 mg/mL collagenase A, and 0.1% trypsin (Gibco) for 30 minutes at 37°C. Cells were passed through a 40-μm cell strainer (Falcon), washed 3 times, and seeded in Dulbecco's modified Eagle's medium (DMEM)/F12 (Gibco) supplemented with 20 ng/mL basic fibroblast growth factor (bFGF) (Invitrogen), 20 ng/mL EGF (Invitrogen), B-27 supplement (1:50 dilution, Invitrogen), and 4 ug/mL heparin on ultra-low attachment plates (Corning Inc.) to grow them as mammospheres. Established mammospheres were plated in cluster plates in DMEM/F12 culture medium [with 10% FBS, 5% penicillin–streptomycin (Gibco), 5 μg/mL insulin (Sigma), 5 ng/mL EGF (Invitrogen), and 5 ng/mL cholera toxin (Sigma)] under low-oxygen (3%) conditions to obtain epithelial cell populations. All mammosphere-derived BRCA1-deficient cell lines were continuously cultured under low-oxygen conditions.

Trp53bp1 *Knockdown*

Brca1$^{\Delta/\Delta}$;*p53*$^{\Delta/\Delta}$ cell lines (KB1P-B11 and KB1P-G3) were transduced with lentiviral pLKO.1-puro vectors containing nontargeting shRNA (SHC002; Sigma) or one of the *Trp53bp1*-targeting hairpins (TRCN0000081778 and TRCN0000081781) from the Sigma MISSION library. Infected cells were selected by growth in medium containing 2 μg/mL (B11) or 3 μg/mL (G3) puromycin for 2 weeks.

Reconstitution of Trp53bp1

For transfection of pCMH6K- *Trp53bp1* (a gift from K. Iwabuchi, Kanazawa Medical University, Ishikawa, Japan), 1 μg DNA in DMEM was used with Lipofectamine Reagent (Invitrogen) according to the manufacturer's instructions. After 18 to 24 hours, the medium was replaced by complete medium. Hygromycin B (100 μg/mL) was added to the growing cells for 4 days.

Mutation Analysis

Genomic DNA was isolated from frozen tumor pieces and cell pellets with phenol–chloroform and isopropanol precipitation. RNA was extracted from tumor pieces with TRIzol and isopropanol precipitation and from cell pellets with the High Pure RNA Isolation Kit (Roche 11828665001). cDNA was prepared using the First Strand Synthesis System (Invitrogen 18080–051). For sequencing, we used the BigDye Terminator v3.1 Cycle Sequencing Kit (Applied Biosystems). Primers that were used to detect the rearrangement in KB1PM5 and the mutations in KB1PM8, KB1P2, and KB1P8 are depicted in Supplementary Table S2.

Clonogenic Assay

To measure the effect of olaparib on colony-forming capacity, we seeded cells at low density in 6-well plates. The next day, olaparib was added, and the concentration of dimethyl sulfoxide was equalized for every well. After 7 days, the colonies were fixed and stained with Leishman eosin methylene blue solution (Merck 105387). All concentrations were measured in duplicate, and each experiment was done 3 times.

Array Comparative Genomic Hybridization

Genomic DNA was extracted with proteinase K and phenol–chloroform, fragmented, and labeled with the Klenow Kit (Roche). Tumor and spleen samples were labeled with the NimbleGen Dual-Color DNA Labeling Kit and hybridized to NimbleGen 12-plex 135K full genome mouse custom NKI array. The data are analyzed with NimbleScan software.

Supplementary Material

Refer to Web version on PubMed Central for supplementary material.

Acknowledgments

The authors thank Anton Berns and Peter Bouwman for critical reading of the manuscript, Susan Bates from the NIH (Bethesda, MD) for providing tariquidar, and Thijs Siegenbeek van Heukelom and Marieke Haenen for technical support.

Grant Support

This work was supported by grants from the Netherlands Organization for Scientific Research (NWO-Toptalent 021.002.104 to J.E. Jaspers and NWO-VIDI-91711302 to S. Rottenberg), the Dutch Cancer Society (projects NKI 2006-3566, NKI 2007-3772, NKI 2009-4303, and NKI 2011-5220), the European Union (EU) FP6 Integrated Project 037665-CHEMORES, the EU FP7 Project 260791-Eurocan-Platform, CTMM Breast Care, and the NKI-AVL Cancer Systems Biology Centre.

REFERENCES

1. Bryant HE, Schultz N, Thomas HD, Parker KM, Flower D, Lopez E, et al. Specific killing of BRCA2-deficient tumours with inhibitors of poly(ADP-ribose) polymerase. Nature 2005;434:913–7. [PubMed: 15829966]
2. Farmer H, McCabe N, Lord CJ, Tutt AN, Johnson DA, Richardson TB, et al. Targeting the DNA repair defect in BRCA mutant cells as a therapeutic strategy. Nature 2005;434:917–21. [PubMed: 15829967]
3. McCabe N, Turner NC, Lord CJ, Kluzek K, Bialkowska A, Swift S, et al. Deficiency in the repair of DNA damage by homologous recombination and sensitivity to poly(ADP-ribose) polymerase inhibition. Cancer Res 2006;66:8109–15. [PubMed: 16912188]
4. Audeh MW, Carmichael J, Penson RT, Friedlander M, Powell B, Bell-McGuinn KM, et al. Oral poly(ADP-ribose) polymerase inhibitor olaparib in patients with BRCA1 or BRCA2 mutations and recurrent ovarian cancer: a proof-of-concept trial. Lancet 2010;376:245–51. [PubMed: 20609468]
5. Evers B, Schut E, van der Burg E, Braumuller TM, Egan DA, Holstege H, et al. A high-throughput pharmaceutical screen identifies compounds with specific toxicity against BRCA2-deficient tumors. Clin Cancer Res 2010;16:99–108. [PubMed: 20008842]
6. Fong PC, Boss DS, Yap TA, Tutt A, Wu P, Mergui-Roelvink M, et al. Inhibition of poly(ADP-ribose) polymerase in tumors from BRCA mutation carriers. N Engl J Med 2009; 361:123–34. [PubMed: 19553641]
7. Hay T, Matthews JR, Pietzka L, Lau A, Cranston A, Nygren AO, et al. Poly(ADP-ribose) polymerase-1 inhibitor treatment regresses autochthonous Brca2/p53-mutant mammary tumors in vivo and delays tumor relapse in combination with carboplatin. Cancer Res 2009;69:3850–5. [PubMed: 19383921]
8. Menear KA, Adcock C, Boulter R, Cockcroft XL, Copsey L, Cranston A, et al. 4-[3-(4-cyclopropanecarbonylpiperazine-1-carbonyl)-4fluorobenzyl]-2H-phth alazin-1-one: a novel bioavailable inhibitor of poly(ADP-ribose) polymerase-1. J Med Chem 2008;51:6581–91. [PubMed: 18800822]
9. Rottenberg S, Jaspers JE, Kersbergen A, van der Burg E, Nygren AO, Zander SA, et al. High sensitivity of BRCA1-deficient mammary tumors to the PARP inhibitor AZD2281 alone and in

combination with platinum drugs. Proc Natl Acad Sci U S A 2008;105:17079–84. [PubMed: 18971340]

10. Tutt A, Robson M, Garber JE, Domchek SM, Audeh MW, Weitzel JN, et al. Oral poly(ADP-ribose) polymerase inhibitor olaparib in patients with BRCA1 or BRCA2 mutations and advanced breast cancer: a proof-of-concept trial. Lancet 2010;376:235–44. [PubMed: 20609467]
11. Liu X, Holstege H, van der Gulden H, Treur-Mulder M, Zevenhoven J, Velds A, et al. Somatic loss of BRCA1 and p53 in mice induces mammary tumors with features of human BRCA1-mutated basal-like breast cancer. Proc Natl Acad Sci U S A 2007;104:12111–6. [PubMed: 17626182]
12. Rottenberg S, Nygren AO, Pajic M, van Leeuwen FW, van der Heijden I, van de Wetering K, et al. Selective induction of chemotherapy resistance of mammary tumors in a conditional mouse model for hereditary breast cancer. Proc Natl Acad Sci U S A 2007;104:12117–22. [PubMed: 17626183]
13. Borst P Cancer drug pan-resistance: pumps, cancer stem cells, quiescence, epithelial to mesenchymal transition, blocked cell death pathways, persisters or what? Open Biol 2012;2:120066. [PubMed: 22724067]
14. Drost R, Bouwman P, Rottenberg S, Boon U, Schut E, Klarenbeek S, et al. BRCA1 RING function is essential for tumor suppression but dispensable for therapy resistance. Cancer Cell 2011;20:797–809. [PubMed: 22172724]
15. Edwards SL, Brough R, Lord CJ, Natrajan R, Vatcheva R, Levine DA, et al. Resistance to therapy caused by intragenic deletion in BRCA2. Nature 2008;451:1111–5. [PubMed: 18264088]
16. Sakai W, Swisher EM, Karlan BY, Agarwal MK, Higgins J, Friedman C, et al. Secondary mutations as a mechanism of cisplatin resistance in BRCA2-mutated cancers. Nature 2008;451:1116–20. [PubMed: 18264087]
17. Norquist B, Wurz KA, Pennil CC, Garcia R, Gross J, Sakai W, et al. Secondary somatic mutations restoring BRCA1/2 predict chemotherapy resistance in hereditary ovarian carcinomas. J Clin Oncol 2011;29:3008–15. [PubMed: 21709188]
18. Swisher EM, Sakai W, Karlan BY, Wurz K, Urban N, Taniguchi T. Secondary BRCA1 mutations in BRCA1-mutated ovarian carcinomas with platinum resistance. Cancer Res 2008; 68:2581–6. [PubMed: 18413725]
19. Schinkel AH, Mayer U, Wagenaar E, Mol CA, van Deemter L, Smit JJ, et al. Normal viability and altered pharmacokinetics in mice lacking mdr1-type (drug-transporting) P-glycoproteins. Proc Natl Acad Sci U S A 1997;94:4028–33. [PubMed: 9108099]
20. Schinkel AH, Smit JJ, van Tellingen O, Beijnen JH, Wagenaar E, van Deemter L, et al. Disruption of the mouse mdr1a P-glycoprotein gene leads to a deficiency in the blood-brain barrier and to increased sensitivity to drugs. Cell 1994;77:491–502. [PubMed: 7910522]
21. Bouwman P, Aly A, Escandell JM, Pieterse M, Bartkova J, van der Gulden H, et al. 53BP1 loss rescues BRCA1 deficiency and is associated with triple-negative and BRCA-mutated breast cancers. Nat Struct Mol Biol 2010;17:688–95. [PubMed: 20453858]
22. Bunting SF, Callen E, Wong N, Chen HT, Polato F, Gunn A, et al. 53BP1 inhibits homologous recombination in Brca1-deficient cells by blocking resection of DNA breaks. C ell 2010;141:243–54.
23. Zander SA, Kersbergen A, van der Burg E, de Water N, van Tellingen O, Gunnarsdottir S, et al. Sensitivity and acquired resistance of BRCA1;p53-deficient mouse mammary tumors to the topoisomerase I inhibitor topotecan. Cancer Res 2010;70:1700–10. [PubMed: 20145144]
24. Singh A, Settleman J. EMT, cancer stem cells and drug resistance: an emerging axis of evil in the war on cancer. Oncogene 2010;29:4741–51. [PubMed: 20531305]
25. Huertas P, Cortes-Ledesma F, Sartori AA, Aguilera A, Jackson SP. CDK targets Sae2 to control DNA-end resection and homologous recombination. Nature 2008;455:689–92. [PubMed: 18716619]
26. Huertas P, Jackson SP. Human CtIP mediates cell cycle control of DNA end resection and double strand break repair. J Biol Chem 2009;284:9558–65. [PubMed: 19202191]
27. Yun MH, Hiom K. CtIP-BRCA1 modulates the choice of DNA double-strand-break repair pathway throughout the cell cycle. Nature 2009;459:460–3. [PubMed: 19357644]
28. Helleday T The underlying mechanism for the PARP and BRCA synthetic lethality: clearing up the misunderstandings. Mol Oncol 2011;5:387–93. [PubMed: 21821475]

29. Bunting SF, Callen E, Kozak ML, Kim JM, Wong N, Lopez-Contreras AJ, et al. BRCA1 functions independently of homologous recombination in DNA interstrand crosslink repair. Mol Cell 2012; 46:125–35. [PubMed: 22445484]
30. Schlacher K, Wu H, Jasin M. A distinct replication fork protection pathway connects Fanconi anemia tumor suppressors to RAD51-BRCA1/2. Cancer Cell 2012;22:106–16. [PubMed: 22789542]
31. Garcia-Higuera I, Taniguchi T, Ganesan S, Meyn MS, Timmers C, Hejna J, et al. Interaction of the Fanconi anemia proteins and BRCA1 in a common pathway. Mol Cell 2001;7:249–62. [PubMed: 11239454]
32. Vandenberg CJ, Gergely F, Ong CY, Pace P, Mallery DL, Hiom K, et al. BRCA1-independent ubiquitination of FANCD2. Mol Cell 2003;12:247–54. [PubMed: 12887909]
33. Patel AG, Sarkaria JN, Kaufmann SH. Nonhomologous end joining drives poly(ADP-ribose) polymerase (PARP) inhibitor lethality in homologous recombination-deficient cells. Proc Natl Acad Sci U S A 2011;108:3406–11. [PubMed: 21300883]
34. Navin N, Kendall J, Troge J, Andrews P, Rodgers L, McIndoo J, et al. Tumour evolution inferred by single-cell sequencing. Nature 2011;472:90–4. [PubMed: 21399628]
35. Li X, Delzer J, Voorman R, de Morais SM, Lao Y. Disposition and drug-drug interaction potential of veliparib (ABT-888), a novel and potent inhibitor of poly(ADP-ribose) polymerase. Drug Metab Dispos 2011;39:1161–9. [PubMed: 21436403]
36. Ledermann JA, Harter P, Gourley C, Friedlander M, Vergote IB, Rustin GJS, et al. Phase II randomized placebo-controlled study of olaparib (AZD2281) in patients with platinum-sensitive relapsed serous ovarian cancer (PSR SOC). J Clin Oncol 29:2011 (suppl; abstr 5003).
37. Bell D, Berchuck A, Birrer M, Chien J, Cramer D, Dao F, et al. Integrated genomic analyses of ovarian carcinoma. Nature 2011;474:609–15. [PubMed: 21720365]
38. Kinders RJ, Hollingshead M, Khin S, Rubinstein L, Tomaszewski JE, Doroshow JH, et al. Preclinical modeling of a phase 0 clinical trial: qualification of a pharmacodynamic assay of poly (ADP-ribose) polymerase in tumor biopsies of mouse xenografts. Clin Cancer Res 2008;14:6877–85. [PubMed: 18980982]
39. National Cancer Institute Division of Cancer Treatment and Diagnosis. Available from: http://dctd.cancer.gov/ResearchResources/biomarkers/docs/par/SOP340520_Biopsy_Tissue.pdf.
40. National Cancer Institute Division of Cancer Treatment and Diagnosis. Available from: http://dctd.cancer.gov/ResearchResources/biomarkers/docs/par/SOP340505_PAR_IA.pdf.

SIGNIFICANCE

In this study, we show that loss of 53BP1 causes resistance to PARP inhibition in mouse mammary tumors that are deficient in BRCA1. We hypothesize that low expression or absence of 53BP1 also reduces the response of patients with BRCA1-deficient tumors to PARP inhibitors.

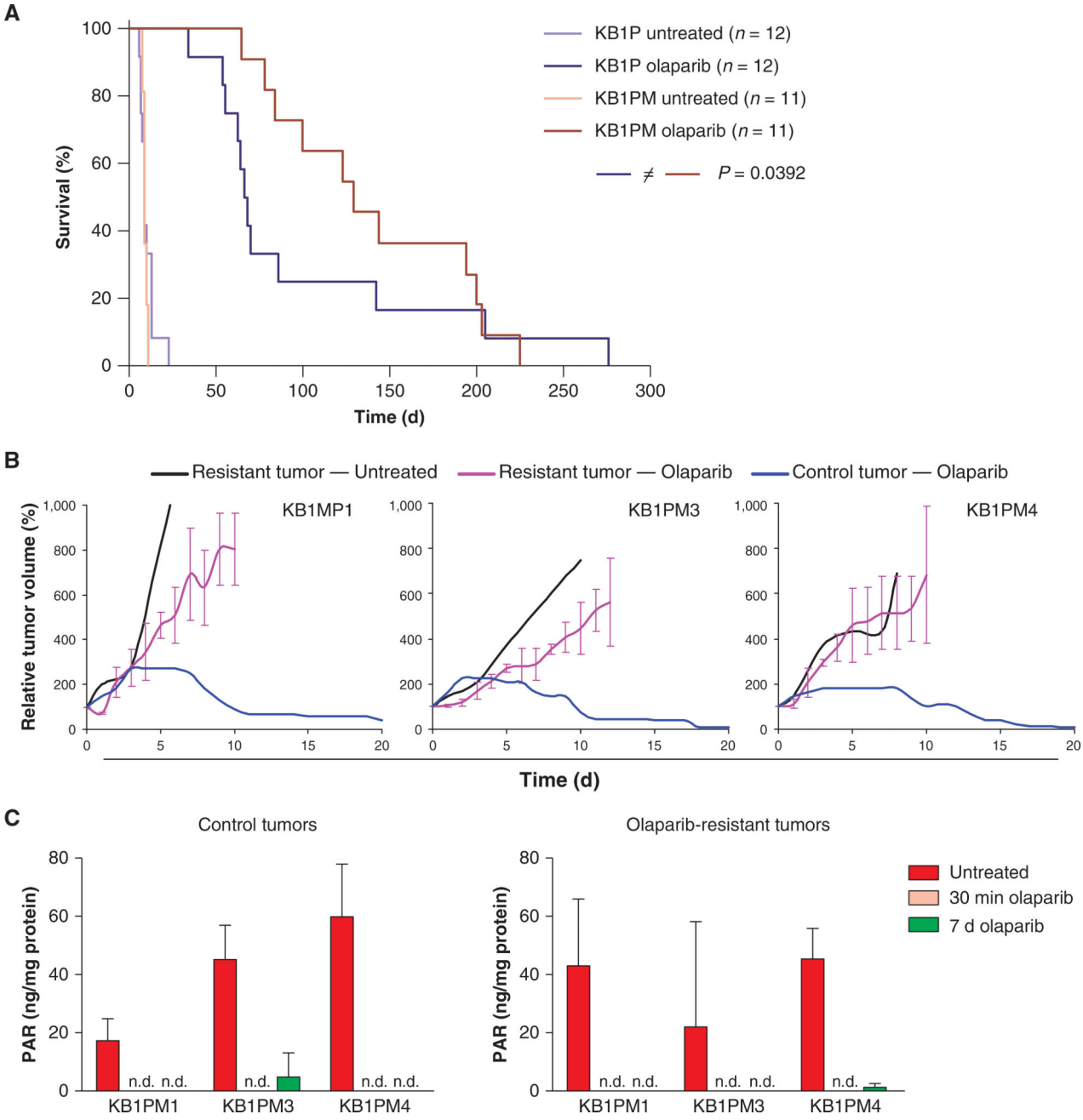

Figure 1.

Acquired resistance of Pgp-deficient *Brca1*$^{\Delta/\Delta}$;*p53*$^{\Delta/\Delta}$ (KB1PM) mouse mammary tumors to the PARPi olaparib. **A,** Kaplan–Meier curve showing survival of mice bearing Pgp-proficient KB1P or Pgp-deficient KB1PM tumors, either untreated or treated with 50 mg/kg olaparib given intraperitoneally for 28 consecutive days. Treatment was resumed when a relapsing tumor reached a size of 100% (the tumor size at the start of the treatment). Individual tumor responses are shown in Supplementary Fig. S1. The Gehan–Breslow–Wilcoxon *P* value is indicated. **B,** response to daily treatment with 50 mg/kg olaparib given intraperitoneally of olaparib-resistant tumors from 3 donor tumors (KB1PM1, 3, and 4) and drug-naïve control

tumors from the corresponding donors. **C,** levels of PAR detected in whole-tumor extracts from olaparib-resistant and control tumors derived from KB1PM1, KB1PM3, and KB1PM4. The tumors were harvested without treatment, 30 minutes after one dose of 50 mg/kg olaparib given intraperitoneally, or 2 hours after the last dose of 7 days of daily treatment. n.d., not detectable (lower than 2*SD above background). Data are presented as mean + SD of 3 mice per donor per treatment.

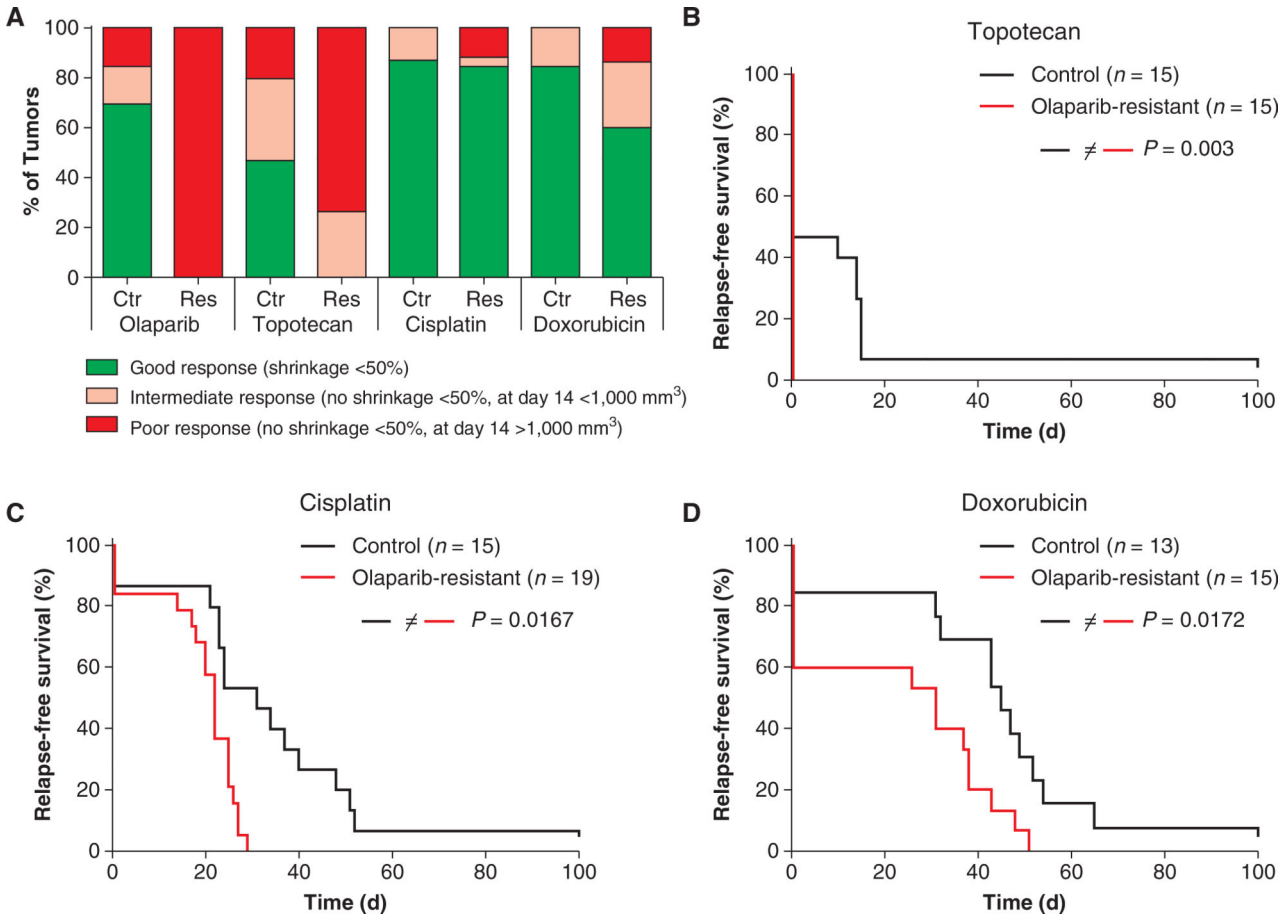

Figure 2.

Response of olaparib-resistant tumors to DNA-damaging agents. **A,** classification of the response of olaparib-resistant (Res) and control tumors (Ctr) from 5 individual donors (KB1PM1, 3, 4, 5, and 8) to olaparib (50 mg/kg, daily for 28 days), topotecan (2 mg/kg, days 0–4 and 14–18), cisplatin (6 mg/kg, day 0), and doxorubicin (5 mg/kg, days 0, 7, and 14). Untreated tumors would be classified as "poor responders." **B –D,** for the same group of mice, the relapse-free survival is shown in response to topotecan, cisplatin, or doxorubicin. The poor and intermediate responders of **A** have a relapse-free survival of 0 days, as the tumor did not shrink below 50% of the original size. Day 0 is the start of the treatment. The Gehan–Breslow–Wilcoxon *P* values are indicated.

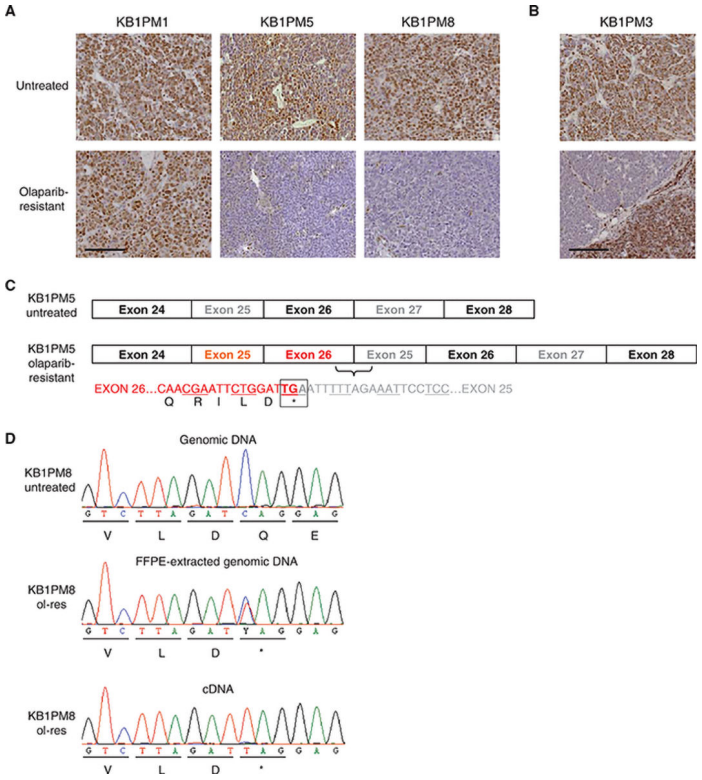

Figure 3.

Loss of 53BP1 protein in olaparib-resistant tumors. **A,** 53BP1 in control and olaparib-resistant KB1PM tumors. Depicted are 2 individual tumors with loss of 53BP1 and one of the olaparib-resistant tumors that still expresses 53BP1. The 53BP1-positive cells in the resistant tumors of KB1PM5 and KB1PM8 are either stroma or a duct from the wild-type host mammary gland. **B,** olaparib-resistant tumor KB1PM3 shows focal loss of 53BP1 expression. **C,** cDNA sequencing revealed a duplication of exons 25 and 26 in *Trp53bp1*, resulting in a frame shift and premature stop codon in the olaparib-resistant tumor cells of KB1PM5. The alternating codons are underlined and the premature stop codon is indicated in bold. **D,** identification of a heterozygous truncating mutation Q626* in exon 12 *Trp53bp1* in the 53BP1-negative areas of olaparib-resistant (ol-res) tumor KB1PM8. cDNA sequencing identified only the mutated allele. Primers that were used for KB1PM5 and KB1PM8 are listed in Supplementary Table S2. FFPE, formalin-fixed, paraffin-embedded. Scale bar, 100 μm.

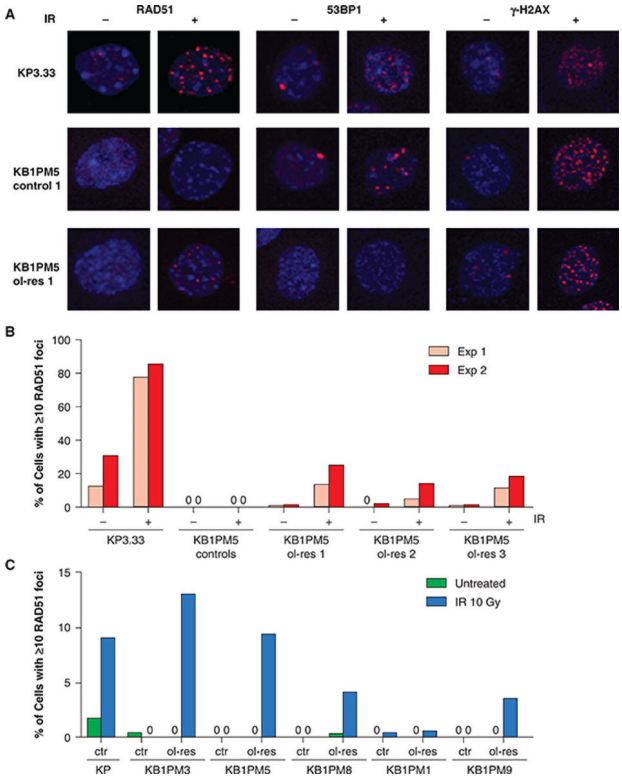

Figure 4.

DNA damage foci in irradiated cells. **A,** detection of ionizing radiation–induced RAD51, 53BP1, and γ-H2AX foci in BRCA1-proficient KP3.33 cells (5), a cell line derived from a KB1PM5 control tumor (control 1) and a 53BP1-negative cell line derived from the olaparib-resistant KB1PM5 tumor (ol-res 1). For characterization of the cell lines, see also Supplementary Fig. S5. Images show the maximum projection, covering the whole cell in the z-direction. **B,** quantification of RAD51 focus formation of 3 KB1PM5 control cell lines and 3 KB1PM5 olaparib-resistant cell lines in 2 independent experiments. The 3 control cell lines are combined in one bar, and each olaparib-resistant cell line is shown separately for both experiments. **C,** quantification of RAD51 IRIFs in a control KP tumor and in matched olaparib-sensitive and -resistant KB1PM tumors. See also Supplementary Fig. S6. IR, ionizing radiation.

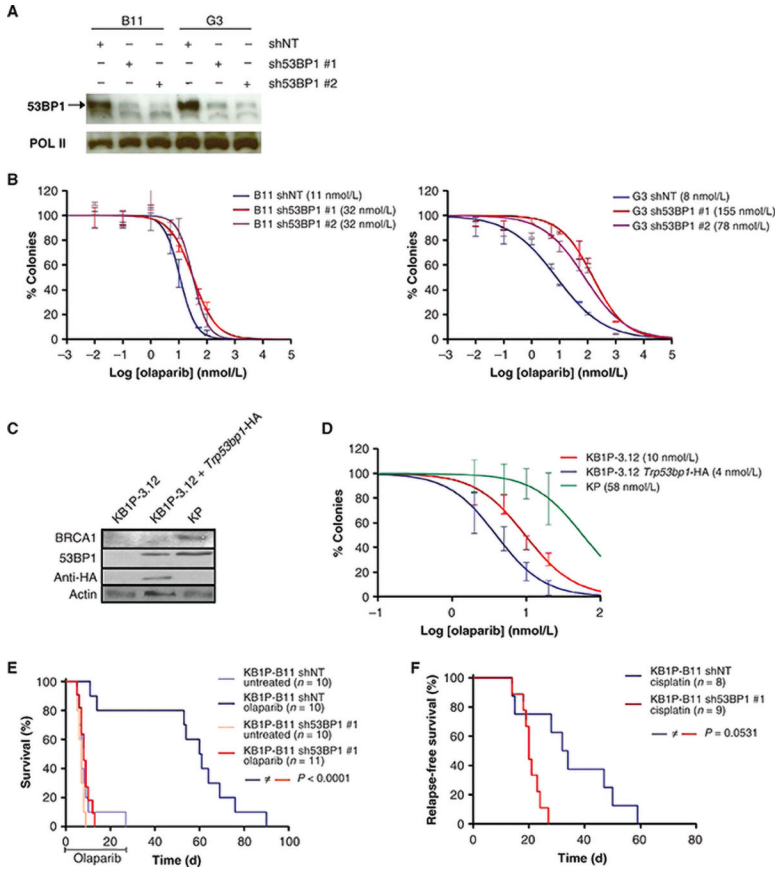

Figure 5.

The effect of 53BP1 loss on olaparib sensitivity. **A,** Western blot analysis showing 53BP1 levels in KB1P-B11 and KB1P-G3 cells that express a nontargeting hairpin (NT) or a hairpin against *Trp53bp1*. **B,** clonogenic assay with olaparib. The IC_{50} is indicated between brackets. **C,** Western blot analysis showing the reconstitution of 53BP1 in 53BP1-deficient KB1P-3.12 cells. KP cells are used as positive control for the BRCA1 Western blot analysis. **D,** clonogenic assay of 53BP1-negative KB1P-3.12 cells, h53BP1-reconstituted KB1P-3.12 cells, and BRCA-proficient KP cells. **E,** overall survival of mice with a 53BP1-positive (shNT) or -negative (sh53BP1) tumor treated with one regimen of olaparib daily for 28 days and the untreated control mice. 53BP1 expression in these tumors is shown in Supplementary Fig. S7C. **F,** relapse-free survival of mice with a 53BP1-positive (shNT) or negative (sh53BP1) tumor treated with one dose of cisplatin. The Gehan–Breslow–Wilcoxon *P* values are indicated.

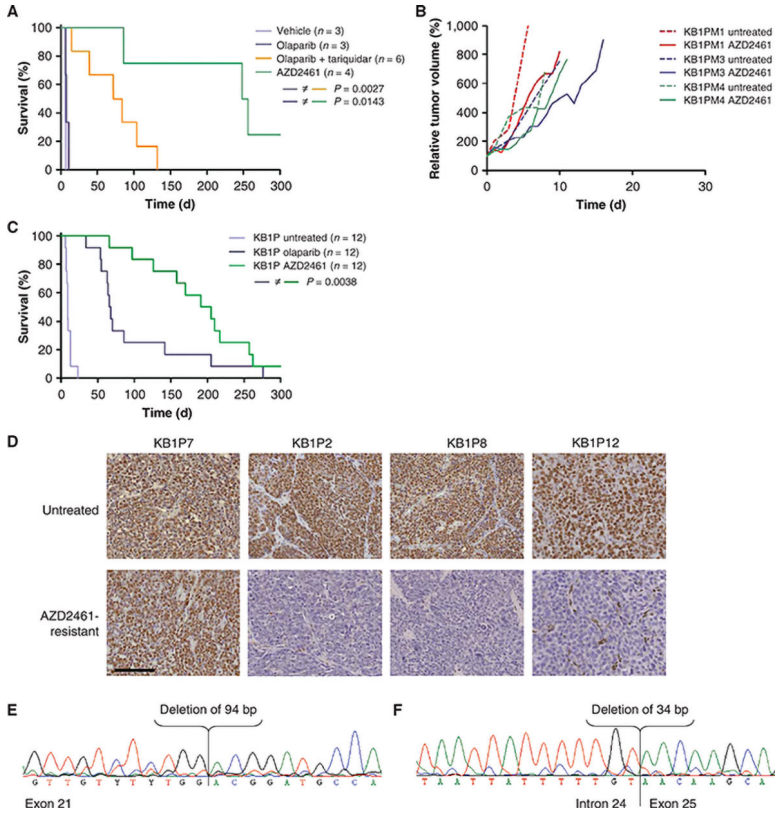

Figure 6.

Non–Pgp-mediated resistance to the next generation PARPi AZD2461. **A,** overall survival of mice with an olaparib-resistant KB1P tumor, with 80-fold increase in *Mdr1b* expression, that were treated with the vehicle of AZD2461 (0.5% v/w HPMC), olaparib, olaparib in combination with the Pgp inhibitor tariquidar, or with AZD2461. **B,** tumor growth of the Pgp-deficient, olaparib-resistant tumors from KB1PM1, KB1PM3, and KB1PM4, either untreated or treated with AZD2461. **C,** Kaplan–Meier curve showing survival of mice with a Pgp-proficient KB1P tumor, either untreated or after treatment with olaparib or AZD2461. Individual tumor responses are shown in Supplementary Figs. S1C and S9C. The Gehan–Breslow–Wilcoxon *P* value is indicated. **D,** 53BP1 in control and AZD2461-resistant KB1P tumors. Depicted are 3 individual tumors with loss of 53BP1 and one of the AZD2461-resistant tumors that still express 53BP1. Scale bar, 100 μm. **E,** identification of a 94-bp deletion in exon 21 of *Trp53bp1* in AZD2461-resistant tumor KB1P2, leading to a frame shift and early stop codon in exon 21. **F,** identification of a 34-bp deletion at the splice acceptor site of exon 25 of *Trp53bp1*.

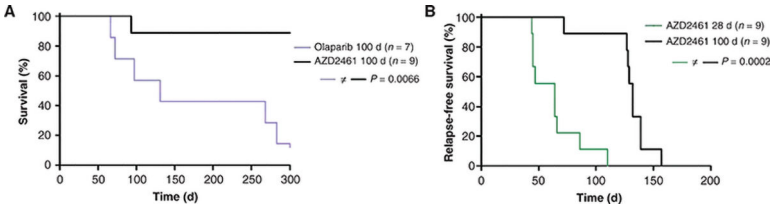

Figure 7.

Chronic antitumor efficacy of the novel PARPi AZD2461. **A,** overall survival of mice receiving 100 days of olaparib (see also ref. 9) or AZD2461 treatment. After relapse of a tumor to a size of 100%, treatment was given for another 100 days. Individual tumor responses are shown in Supplementary Fig. S10A–S10C. **B,** relapse-free survival of mice with a KB1P tumor that received AZD2461 for 28 consecutive days or for 100 consecutive days. The Gehan–Breslow–Wilcoxon *P* values are indicated.